Annals of Phytomedicine 14(1): 1053-1064, 2025

DOI: http://dx.doi.org/10.54085/ap.2025.14.1.105

Annals of Phytomedicine: An International Journal
http://www.ukaazpublications.com/publications/index.php

Print ISSN : 2278-9839 Online ISSN : 2393-9885

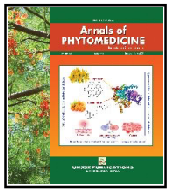

Original Article : Open Access

# Isolation and characterization of antibacterial γ-Muurolene from *Ischnoderma resinosum* (Schrad.) P. Karst.: Phytochemical analysis and efficacy against pathogenic bacteria

**R. Kadhar Nivas*, K. Bhanumathi**, C. Ramalakshmi***, R. Mariselvam****◆, S. Thanga Parameshwari***** and S. Ananthi********

**Department of Biotechnology, EGS Pillay Arts and Science College (Autonomous), Nagapattinam-611002, Tamil Nadu, India*
*** Department of Zoology, Kamaraj College, Thoothukudi-628003, Tamil Nadu, India*
**** Department of Food and Nutrition, St. Eugene University, Chibombo-330081, Zambia*
***** Centre of Molecular Medicine and Diagnostics (COMManD), Department of Biochemistry, Saveetha Dental College and Hospitals, Saveetha Institute of Medical and Technical Sciences, Saveetha University, Chennai-600077, India*
****** Tamil Institute of Science and Technology, Seeniyapuram, Tenkasi-627423, Tamil Nadu, India*
******* Clinbiocare Technology, Mathalamparai, Tenkasi-627 814, Tamil Nadu, India*

**Article Info**

**Article history**
Received 13 April 2025
Revised 28 May 2025
Accepted 29 May 2025
Published Online 30 June 2025

**Keywords**
*Ischnoderma resinosum* (Schrad.) P. Karst.,
Bioactive components
GC-MS
Antibacterial activity
Molecular docking

**Abstract**

In recent days, the uses of macro fungi have suddenly increased worldwide due to their nutritional and nutraceutical applications. In this study, we isolated and characterized the active molecule from macro fungus *Ischnoderma resinosum* (Schrad.) P.Karst. and studied the antibacterial activity for crude extract and isolated molecule. The phytochemical profile was done through GC-MS. 29 dominant compounds are presented in the mushroom based methanol extract. Active molecules were isolated and characterized by UV/Vis spectrophotometer, FT-IR, 1H NMR and 13C NMR. Based on the spectral characterization, the isolated molecule is γ-Muurolene. The mushroom γ-Muurolene molecule reveled an excellent antibacterial molecule against *Bacillus subtilis*, *Enterobacter* spp. and *Staphylococcus aureus*. Molecular docking studies were conducted to investigate the interaction between the bioactive compound γ-Muurolene and the target receptor protein EndoA (PDB ID: 6ZDF). The analysis revealed the formation of significant hydrophobic interactions with key amino acid residues, including Arg143, Asn145, Asn124, Pro114, Pro146, Tyr120, Lys119, and Gln115. These interactions suggest a potential binding affinity of γ-Muurolene to EndoA, which contribute to its antibacterial activity.

## 1. Introduction

Fungi are vital organisms of fundamental importance to life on Earth. Epigeous fruiting bodies of fungi, visible to the naked eye, are called mushrooms (Ganeshpurkar *et al*., 2010). Mushrooms used as medicines for 5000 years or more by human beings (Zhang *et al*., 2016). People can certainly obtain health uses simply from adding different mushrooms. It good sources of B vitamins, fiber, and antioxidants to the human diet (Romm 2010). The mushroom bioactive metabolites remarkable function as antibacterial (Gebreyohannes *et al*., 2019), antifungal (Liu *et al*., 2020), antiviral (Sillapachaiyaporn and Chuchawankul, 2020), antioxidants, anticancer, anti-inflammation, hypocholesterolemic (Cheung, 1996), immuno suppressive (Li *et al*., 2013), and immunostimulant properties (Nandi *et al*., 2014). The usage of mushroom based natural molecules were increased their applicability in the society for treating many diseases like cancer, cardiovascular (Mehra *et al*., 2020), neurodegenerative, *etc*. Only few mushrooms were identified as medicinal and they were cultivated for their usage in globally. Many wild mushrooms are unidentified and they have hidden secret. Wild mushrooms, which are suitable for human consumption and which can be benefited as medicine. Constitute an alternative source for human utility. Many chemical drugs against various diseases such as cancer can be detained from them part from their use as nutraceticals. The research by some scientists from Japan and China suggested that mushrooms improved the disease-free intervals and overall survival in breast cancer patients by immune modulation (Szarka *et al*., 1994). Mushrooms have huge nutritional and therapeutic biocomponents that validate their convention in maintaining worldwide communal health (Abdel-Azeem *et al*., 2019). The therapeutic uses of mushrooms have been established through intensive research conducted worldwide. Mushrooms are used in the form of extracts or powder for anticipation, alleviation, or healing of multiple diseases, and/or in complementary a healthy diet (Marcus 2013). There are more than 130 therapeutic functions produced by medicinal mushrooms. Many species of mushrooms are used in traditional medicine, but the following are the most valuable: *Ganoderma lucidum* (Kumar *et al*., 2020), *Lentinus edodes* (Sknepnek *et al*., 2020), *Trametes versicolor* (Kim *et al*., 2002), *Schizophyllum commune* (Basso *et al*., 2020), *Flammulina velutipes* (Xiao *et al*., 2020), *Pleurotus ostreatus* (Kózka *et al*., 2020), *Agaricus bisporus*

**Corresponding author: Dr. R. Mariselvam**
*Adjunct Faculty, Centre of Molecular Medicine and Diagnostics (COMManD), Department of Biochemistry, Saveetha Dental College and Hospitals, Saveetha Institute of Medical and Technical Sciences, Saveetha University, Chennai-600077, Tamil Nadu, India*
**E-mail: r.mariselvam@silsorg.in; honeyselvam01@gmial.com**
**Tel.: +91-8012261469**

(Kozarski *et al*., 2011), *A. brasiliensis* (Kozarski *et al*., 2011), *Tricholoma matsutake* (Ding and Hou, 2012), *Auricularia* sp. (Liang *et al*., 2019), *Grifola frondosa* (Yu *et al*., 2020), *Cordyceps sinensis* (Su , 2019), *Coprinus comatus* (Gao *et al*., 2021), *Inonotus obliquus* (Zhao and Zheng 2021), *Phellinus linteus* (Reis *et al*., 2014), *Laetiporus sulphureus* (Khalilov *et al*., 2019) and *Hericium erinaceus* (He *et al*., 2017). The Western Ghats region of India constitutes a major hotspot of diversity of wild mushrooms. Especially Coutrallam hills have most suitable climate conditions due to North East monsoon and South west monsoon for wild mushroom growth. The Coutrallam hills are uncovered area and suitable for various wild mushrooms. These mushrooms are unexplored will be able to potential therapeutic effects. In this regards, the present study deals with the extraction of active molecules from these unexplored wild mushroom. *Ischnoderma* species were collected from Coutrallam hills, Southern Western Ghats such aspects explicitly for their phytochemical profile and antimicrobial property.

## 2. Materials and Methods

### 2.1 Mushroom collection

The wild macro fungi were collected from the Coutrallam hills in the month of December 2019 in the range of latitude 8.93623° N and longitude 77.30716° E with the altitude of 167.64 meters. The mushroom was collected and preserved with the help of proper preservatives at the SILS Herbarium with the Accession No. of MS-29/2019 further studies.

### 2.2 Identification

Morphological characteristics and online mushroom identification tool (Champignouf.org) were used for identification.

### 2.3 Extraction

The collected mushrooms were dried and powdered. The powdered material was extracted by cold extraction technique. The highly polar solvent (Methanol) was used for extraction. The extracts were filtered using Whatmann No 1 filter paper. The excess solvents were removed by rotary vacuum evaporator and water bath. The mushroom crude extract were stored at - 4°C for further studies.

### 2.4 Phytochemical profile of crude extract

Phytochemicals profile was analyzed through GC/MS analysis of the methanolic extract of mushroom extract was carried out using a Perkin Elmer GC Claurus 500 system and Gas chromatograph coupled with mass spectrometer (GC/MS) along with silica capillary column (30 m × 0.25 mm × 1 µm) which made of 100% dimethyl polysiloxane) for identifying active molecules present in the selected mushroom species. The relative percentage quantity of all components was estimated by comparing its average peak area to the total areas. Identification of components was done by National Institute of Standard Technology (NIST) database and Chemical library. The name, molecular weight and structure of each component of mushroom extract were ascertained. Methanol extract were characterized using UV/Visible spectrophotometer 8805.

### 2.5 Isolation of molecules

The crude compounds were stored in cool place without any disruption. Molecules were isolated by slow evaporation techniques.

### 2.6 Characterization of active molecule

The isolated molecule was characterized through UV/V is spec, FT-IR, 1H NMR, and 13C NMR with using standard protocol.

### 2.7 Antimicrobial bioassay studies of crude extract and isolated molecules

The bacterial growth inhibitory efficacy of mushroom extract was tested against five different bacterial pathogens like *Pseudomonas aeruginosa*, *Bacillus subtilis*, *Enterobacter* spp., *Staphylococcus aureus*, and *E. coli* using the well diffusion method. Wells (8 mm in size) were made in agar plates containing bacterial inoculums. The crude extracts and isolated (25, 50, 75 and 100 µl) were added to the wells of the culture plates. Following incubation for 24 h at 37°C, the plates were observed. The zones of inhibition were measured using a Hi Media measuring scale and expressed in millimeters.

### 2.8 Molecular studies

Molecular docking analysis was conducted to evaluate the interaction between the EndoA protein (PDB ID: 6ZDF) and the bioactive compound γ-Muurolene. The protein structure was retrieved from the Protein Data Bank (PDB) and the ligand γ-Muurolene was obtained from PubChem and prepared through energy minimization using molecular modeling tools. The optimized ligand structure was converted into a compatible format for docking. AutoDock Vina was used for docking, where the receptor-ligand interaction was assessed based on binding affinity scores. The docking results were further analyzed using visualization tools such as PyMOL and Discovery Studio, which confirmed the presence of hydrophobic interactions contributing to the ligand's stability within the active site.

## 3. Results

The collected mushroom was preserved with the help of 4% formalin solution and it was stored at the SILS Herbarium with the Accession No. of MS-29/2019. These mushrooms were collected from the tree of *Tamarindus indica* L. (Figures 1a and 1b) in the area of Coutrallam hills. These mushrooms were morphologically distinct "shelves" that ranged in diameter from 5 to 25 cm. A large number of small tubular filaments, or hyphae, make up these shelves. Large brackets are how the mushroom grows. The upper side of young fruiting bodies is dark brown, while the lower side is wet, rubbery, and sulfur-yellow. The brown cubical rot caused by this fungus eventually causes the host tree to fall because it is unable to bend and flex in the wind. Based on the online tool results and their morphological characteristics the collected mushrooms were under the species of *I. resinosum*.

The crude extract of mushrooms UV/Vis absorption spectra (Figure 2) showed that the absorption peaks were in the nanometer-scale ultra violet range of 206, 268, 368, and one valley peak range at 246 nm. The crude extract had one visible absorption peak range at 382 nm. This result indicated that methanol based mushroom crude contains many numbers of molecules are presented.

Phytochemicals profile was analyzed through GC/MS; the methanolic extract of mushroom extract contains 29 active components presented in the test mushroom extract (Figure 3 and Table 1). The 29 components are benzenamine, N,N-diethyl-3-methyl-4-(triphenyl-stannyl)-, furazan-3-carbohydrazide, 4-amino-N2-(2-chloro-5-nitrobenzylideno)-, distannoxane, hexabutyl-, .eta.-pentamethylcy-

clopentadienyl-ethylisonitril-(N,N,N',N'-tetramethylethin-1,2-diamin)-molybdaeniodid, 1,5-methano-1H,7H,11H-furo[3,4-g]pyrano[3,2-b]xanthene-7,15-dione, 3,3a,4,5-tetrahydro-8-hydroxy-1-(4-hydroxy-3-methyl-2-butenyl)-3,3,11,11, 2-methylresorcinol, bis(pentafluoropropionate), germane, (1-methyl-1,2-pentadien-4-yne-1,3,5-triyl)tris[trimethyl-, sarcosine, N-(2-methylbenzoyl)-, tetradecyl ester, benzoyl chloride, 3-methyl-, naphthalene, 1,2,3,4,4a,7-hexahydro-1,6-dimethyl-4-(1-methylethyl)-, succinic acid, butyl 4-trifluoromethylbenzyl ester, 1H-3a,7-methanoazulene, 2,3,4,7,8,8a-hexahydro-3,6,8,8-tetramethyl-, [3R-(3.alpha.,3a.beta.,7.beta.,8a.alpha.)]-, 7-bis (pentafluoropropionyl)amino-4-methylcoumarin, 3,4-di(pentafluo ropropionyloxy) hydrocinnamic acid, benzisoxazole-2-acetic acid, hydrazide, gamma.-muurolene, .beta.-longipinene, aromandendrene, 1H-benzocycloheptene, 2,4a,5,6,7,8,9,9a-octahydro-3,5,5-trimethyl-9-methylene-, (4aS-cis)-, eudesma-4(15),7-dien-1.beta. –ol, diethyl chloromethanephosphonate, cycloisolongifolene, 8,9-dehydro-, naphthalene, 1,2,4a,5,6,8a-hexahydro-4,7-dimethyl-1-(1-methylethyl)-, neoisolongifolene, caryophyllene, beta.-guaiene, 1H-cyclopropa[a]naphthalene, decahydro-1,1,3a-trimethyl-7-methylene-, [1aS-(1a.alpha., 3a.alpha., 7a.beta.,7b.alpha.)]-, aromandendrene, naphthalene, 1,2,4a,5,8,8a-hexahydro-4,7-dimethyl-1-(1-methylethyl)-, and [1S-(1.alpha.,4a.beta.,8a.alpha.)].

The UV/V is spectral data of isolated molecules having two absorption peaks at 205.5 and 270.5nm and one valley peak at 242 nm (Figure 4).

FTIR analysis showed intensive ranges 495.26, 616.51, 689.97, 874.43, 925.14, 1014.44, 1062.14, 1323.74, 1447.54, 2016.67, 2923.79 and 3181.41 $cm^{-1}$. These bands correspond to the different functional molecules present in the isolated molecule (Figure 5 and Table 2).

Figure 6 despite the 1H NMR spectra, the peak at 1.57 ppm in nuclear magnetic resonance (NMR) spectroscopy is likely to be due to the chemical shift of a specific type of nuclei, such as protons (1H). The chemical shift is a measure of the position of a peak in the NMR spectrum and is related to the electronic environment of the nuclei. A peak at 3.65 ppm in 1H NMR is associated with protons in an aromatic ring or an alkyl group with a relatively low electron density. However, it is also important to consider the coupling pattern and the multiplicity of the signal as well as the context of the molecule. A peak at 7.09 ppm could indicate the presence of protons in a molecule that are in a relatively low electron density environment such as a methylene group ($-CH_2-$) or a methyl group ($-CH_3$). A peak at 7.24-7.25 ppm could indicate the presence of protons in a molecule that are in a relatively low electron density environment such as a methylene group ($-CH_2-$) or a methyl group ($-CH_3$). However, it is also important to consider the coupling pattern and the multiplicity of the signal as well as the context of the molecule in order to identify the specific proton and its environment. It can also be an indication of protons in an aliphatic/non-aromatic ring or an alkyl group. A peak at 7.43 ppm could indicate the presence of protons in a molecule that are in a sp3 hybridized carbon or aliphatic/non-aromatic ring. But also it is important to consider the coupling pattern and the multiplicity of the signal as well as the context of the molecule in order to identify the specific proton and its environment.

13C NMR (Figure 7), a peak at 76.89 ppm in a nuclear magnetic resonance (NMR) spectrum would indicate the presence of a specific type of nucleus in the compound being analyzed. In 13C NMR, a peak at 76.89 ppm may be associated with a carbon atom in a sp3 hybridized state and in a specific chemical environment such as in an alkane or alkyl group. A peak at 77.10 ppm would indicate the presence of a specific type of nucleus in the compound being analyzed. The specific nucleus and functional group responsible for the peak would depend on the type of NMR experiment being performed and the compound being analyzed. A peak at 77.31 ppm would indicate the presence of a specific type of nucleus in the compound being analyzed. The specific nucleus and functional group responsible for the peak would depend on the type of NMR experiment being performed and the compound being analyzed. However, generally speaking, chemical shifts in the range of 77.31 ppm are often associated with protons (1H NMR) in certain chemical environments.Based on the spectral data the isolated molecule is gamma-Muurolene (Figure 8) with the molecular formula of $C_{15}H_{24}$.

The mushroom crude extract exhibited good antimicrobial activity against all microbial test cultures (Table 3). The maximum zones of inhibition were observed in 100 µl of extract against *Bacillus subtilis* (22 mM : 2.2 cM), *E. coli* (20 mM : 2.0 cM), *Enterobacter* spp. (18 mM : 1.8 cM) and *Staphylococcus aureus* (17 mM : 1.7 cM) (Figure 9).

The mushroom based isolated molecules exhibited good antimicrobial activity against *Bacillus subtilis, Enterobacter* spp., *Staphylococcus aureus, E. coli* (Table 4). The maximum zones of inhibition were observed in 100 µl of extract against *Bacillus subtilis* (20.33 ± 0.577), *Enterobacter* spp (18.67 ± 0.577), *Staphylococcus aureus* (17 ± 0), and *E. coli* (21.33 ± 0.5773).

Molecular docking analysis was performed to assess the interaction between γ-Muurolene and the target receptor protein EndoA (PDB ID: 6ZDF). The docking study revealed significant hydrophobic interactions between γ-Muurolene and key residues within the active site of EndoA, including Arg143, Asn145, Asn124, Pro114, Pro146, Tyr120, Lys119, and Gln115. These interactions suggest a stable binding conformation of the ligand within the protein's active site (Figure 10).

The binding affinity values obtained from AutoDock Vina ranged from -6.2 kcal/mol to -5.4 kcal/mol, with the best binding mode showing an affinity of -6.2 kcal/mol (Table 5). The root-mean-square deviation (RMSD) values for this mode were 0.000 Å, indicating that this pose represents the most optimal and stable binding conformation. Other docking poses exhibited slightly lower binding affinities, ranging between -5.8 kcal/mol and -5.4 kcal/mol, with varying RMSD values, suggesting alternative binding conformations with lower stability compared to the top-ranked mode.

The molecular docking results indicate that γ-Muurolene exhibits a favorable binding interaction with the EndoA protein. The best docking pose, with a binding energy of -6.2 kcal/mol, suggests a moderate to strong binding affinity, which is primarily stabilized through hydrophobic interactions with key residues within the active site. These interactions are crucial for maintaining the stability of the ligand-receptor complex and potentially influencing the protein's biological activity.

The presence of multiple docking poses with slightly lower binding energies (-5.8 to -5.4 kcal/mol) suggests that γ-Muurolene may adopt

alternative binding conformations, but the stability of these poses is lower compared to the top-ranked mode. The high RMSD values (above 10 Å) for other docking modes indicate that these alternative conformations significantly differ from the best binding mode, suggesting less optimal interactions within the binding pocket.

The observed binding affinity values are comparable to those of known antibacterial compounds, indicating the potential of γ-Muurolene as a promising antibacterial agent. The strong binding affinity and stable interactions with EndoA suggest that γ-Muurolene could potentially interfere with the protein's function, contributing to its antibacterial activity. However, further validation through molecular dynamics simulations and in vitro studies is necessary to confirm the biological significance of these interactions and to explore the potential mechanism of action of γ-Muurolene against pathogenic bacteria.

**Figure 1:** ***I. resinosum*** **upper view (1a); lower view (1b).**

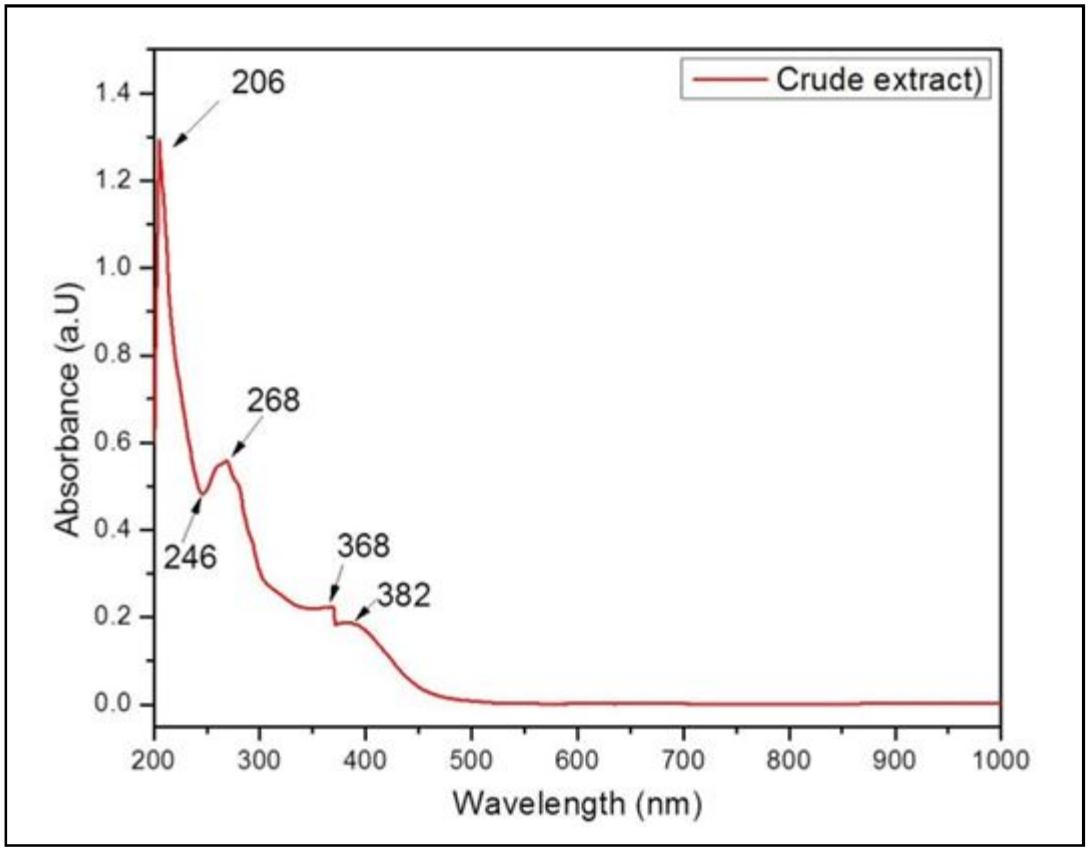


**Figure 2: UV/visible spectrum of** ***I. resinosum*** **methanol extract.**

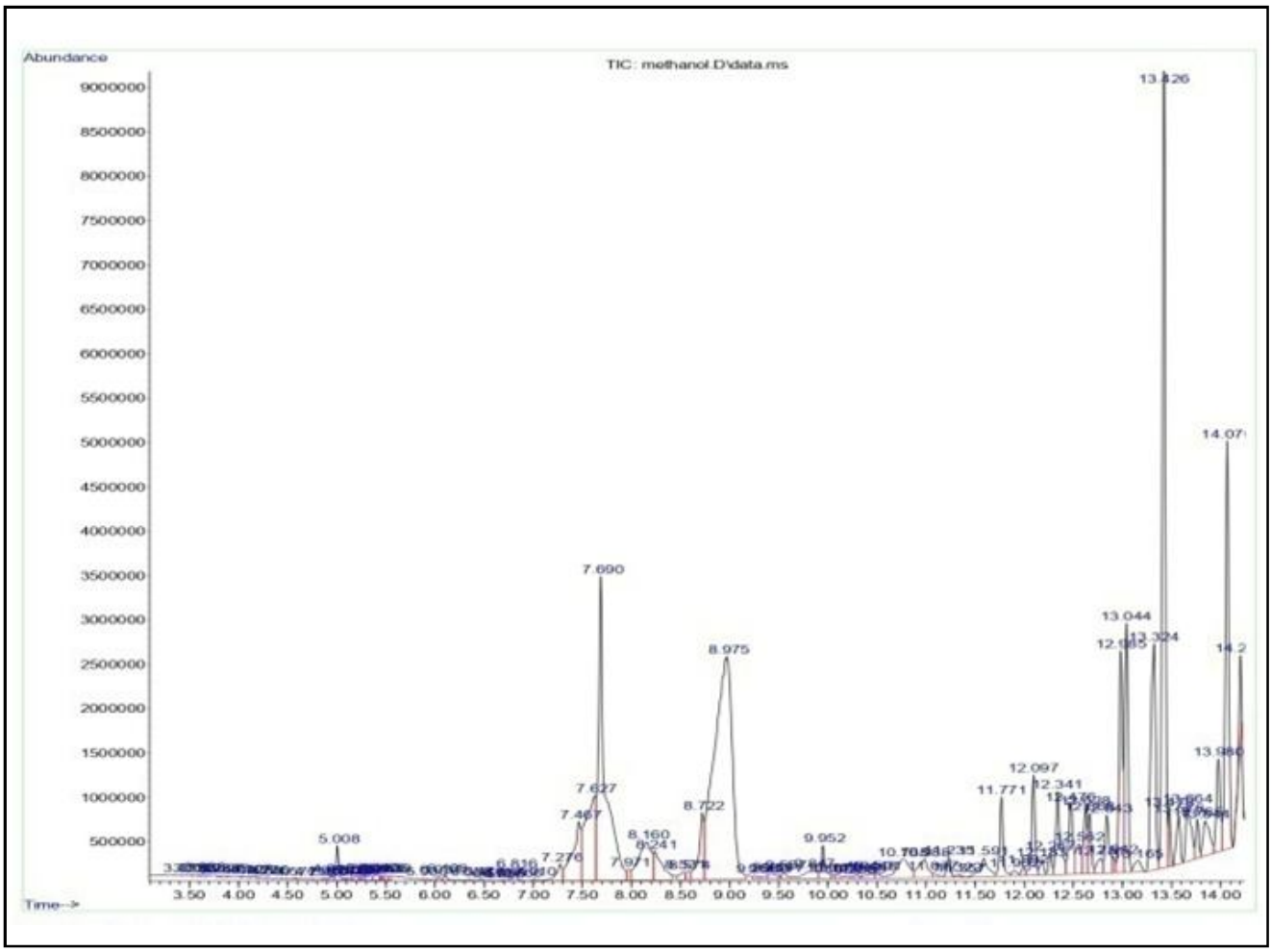


**Figure 3:** GC/MS spectrum of *I. resinosum* methanol extract.

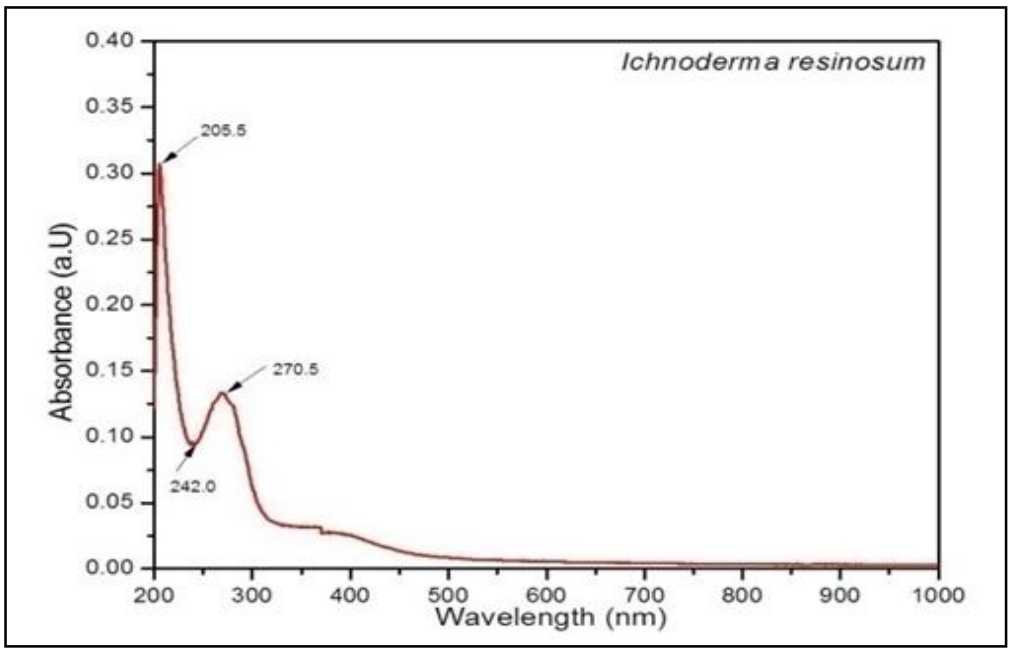


**Figure 4:** UV/Vis spectral characterization of purified compound.

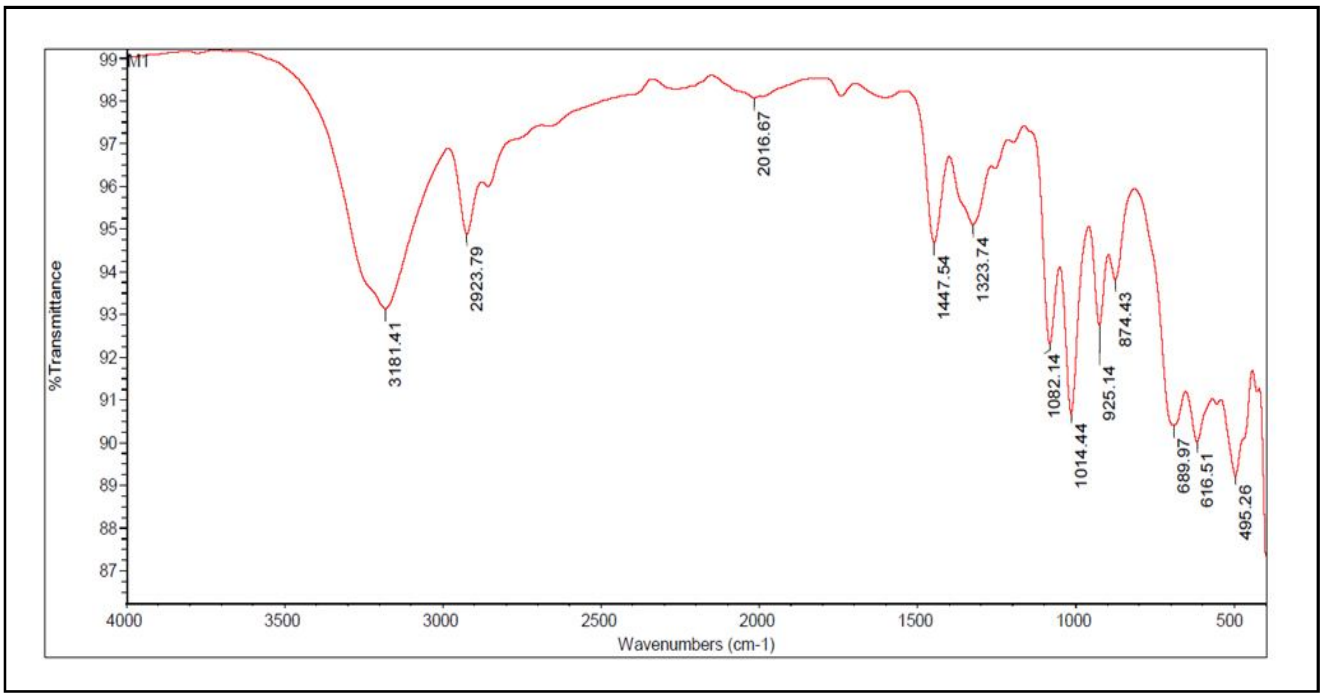


**Figure 5: FTIR characterization of purified compound.**

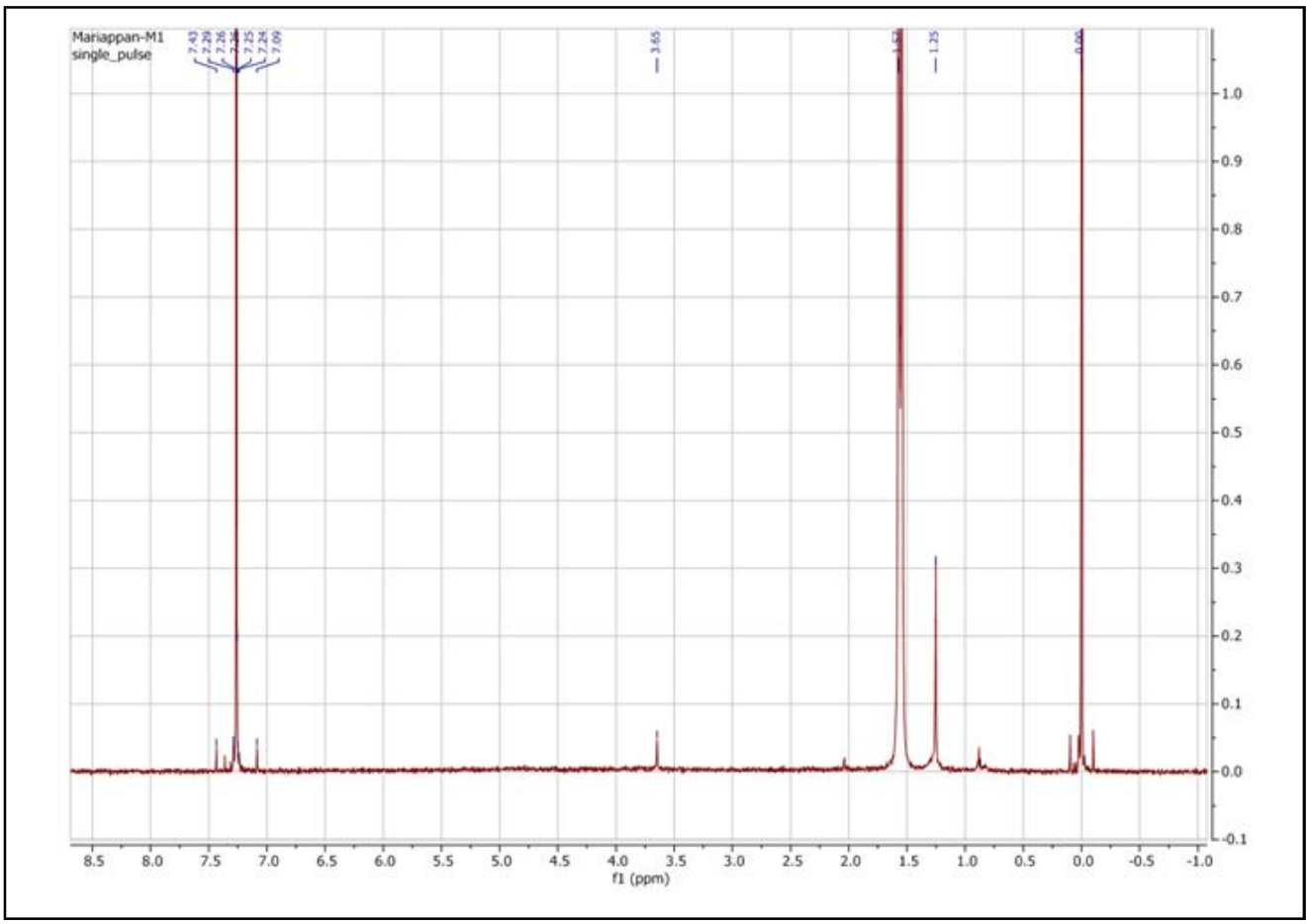


**Figure 6: 1H NMR characterization of purified compound.**

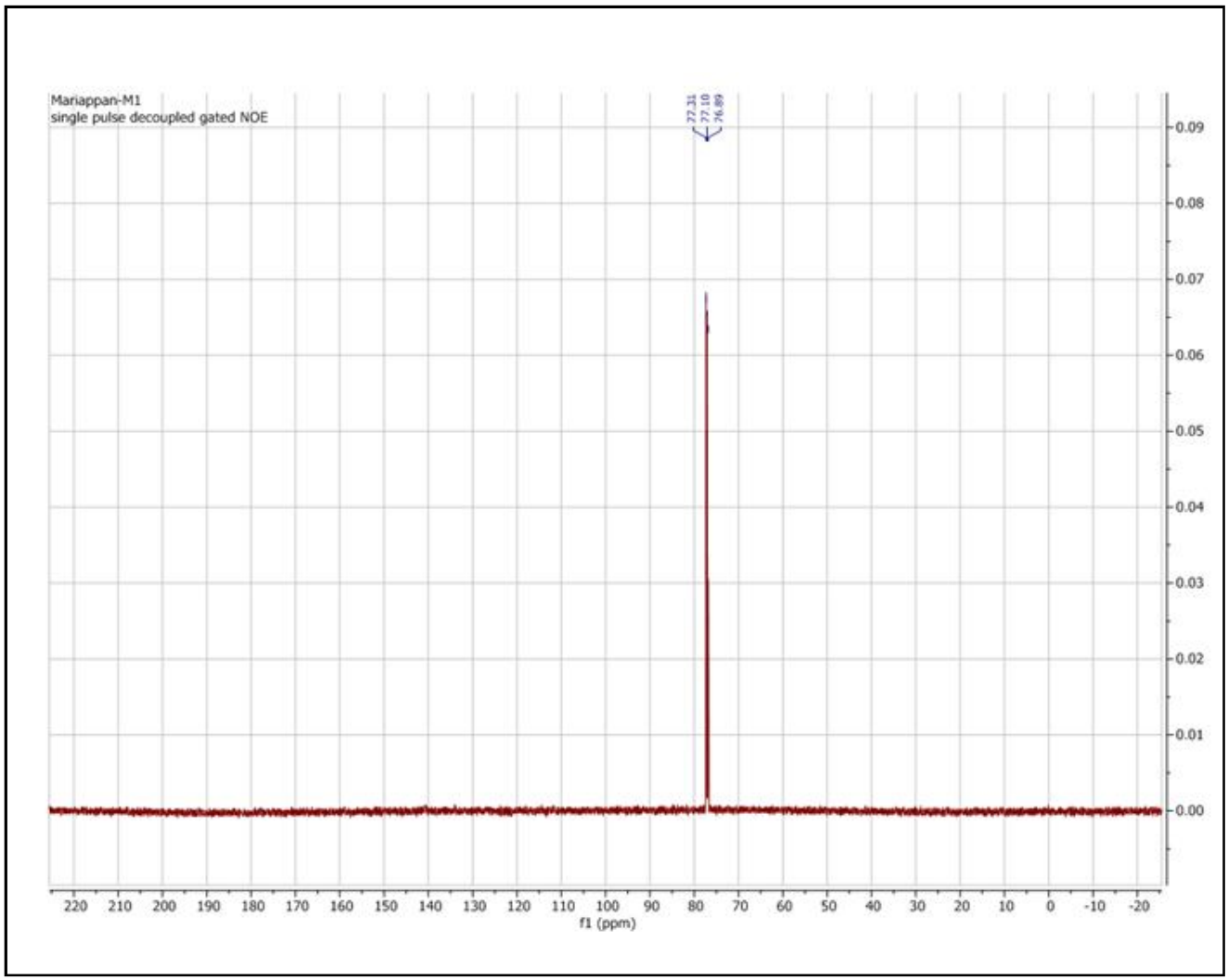


**Figure 7:13C NMR characterization of purified compound.**

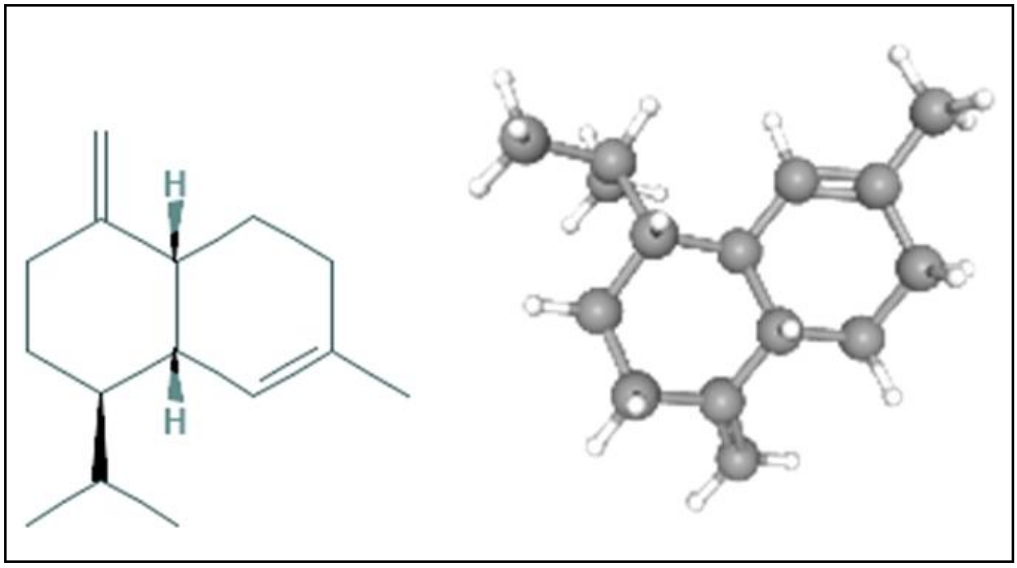


**Figure 8: Isolated molecule (λ-Muurolene).**

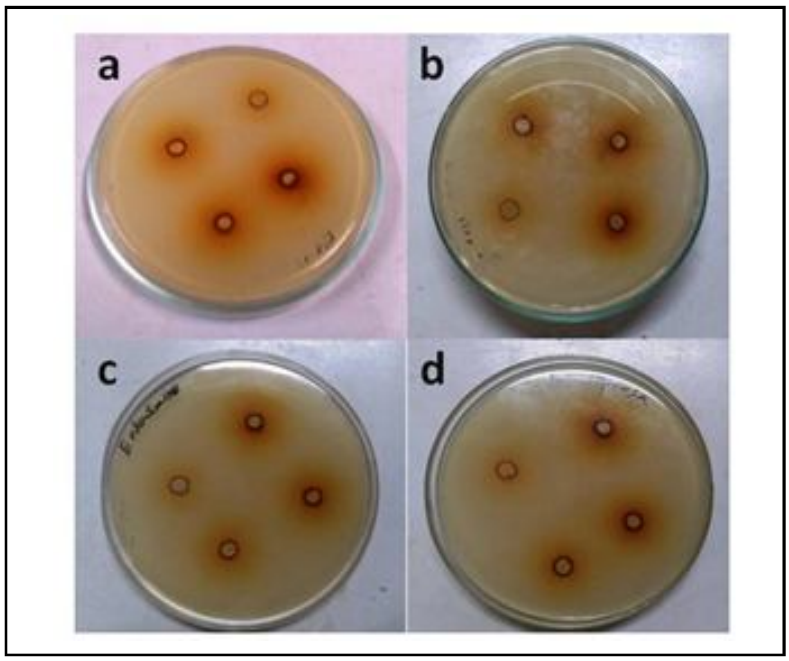


**Figure 9:** Antibacterial assay of *I. resinosum* mushroom extract. a. *E. coli*; b. *Bacillus subtilis*; c. *Enterobacter* spp.; d. *Pseudomonas aeruginosa*.

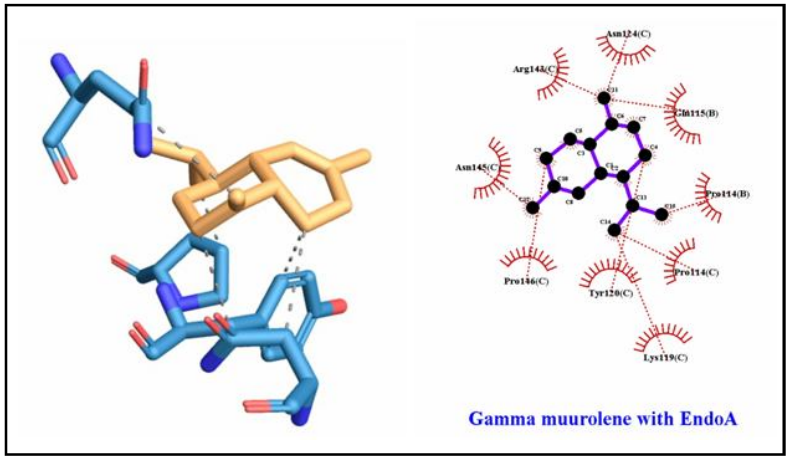


**Figure 10:** *In silico* analysis of γ-Muurolene with Endo A protein.

**Table 1:** GC-MS spectral characterization of *I. resinosum* methanol extract

| S. No. | Proposed compound | RT | Super impossibility |
|---|---|---|---|
| 1 | benzenamine, N, N-diethyl-3-methyl-4-(triphenylstannyl)- | 3.591 | 98.68 |
| 2 | Furazan-3-carbohydrazide, 4-amino-N2-(2-chloro-5-nitrobenzylideno)- | 3.825 | 98.64 |
| 3 | Distannoxane, hexabutyl- | 4.575 | 97.35 |
| 4 | .eta.-Pentamethylcyclopentadienyl-ethylisonitril-(N,N,N',N'-tetramethylethin-1,2-diamin) -molybdaeniodid | 4.947 | 93.67 |
| 5 | 1,5-Methano-1H,7H,11H-furo[3,4-g]pyrano[3,2-b]xanthene-7,15-dione, 3,3a,4,5-tetra hydro-8-hydroxy-1-(4-hydroxy-3-methyl-2-butenyl)-3,3,11,11 | 4.947 | 91.14 |
| 6 | 2-Methylresorcinol, bis(pentafluoropropionate) | 5.078 | 92.28 |
| 7 | Germane, (1-methyl-1,2-pentadien-4-yne-1,3,5-triyl)tris[trimethyl- | 5.101 | 96.67 |
| 8 | Sarcosine | 5.164 | 98.93 |

| | | | |
|---|---|---|---|
| 9 | Benzoyl chloride, 3-methyl- | 5.216 | 90.69 |
| 10 | Naphthalene, 1,2,3,4,4a,7-hexahydro-1,6-dimethyl-4-(1-methylethyl)- | 5.410 | 97.87 |
| 11 | Succinic acid, butyl 4-trifluoromethylbenzyl ester | 5.444 | 99.47 |
| 12 | 1H-3a,7-Methanoazulene, 2,3,4,7,8,8a-hexahydro-3,6,8,8-tetramethyl-, [3R-(3.alpha., 3a.beta.,7.beta.,8a.alpha.)]- | 5.467 | 95.33 |
| 13 | 7-bis(Pentafluoropropionyl)amino-4-methylcoumarin | 5.496 | 95.59 |
| 14 | 3,4-Di(pentafluoropropionyloxy)hydrocinnamic acid | 5.536 | 98.94 |
| 15 | Benzisoxazole-2-acetic acid, hydrazide | 5.902 | 91.81 |
| 16 | gamma-Muurolene | 7.464 | 99.75 |
| 17 | .beta.-Longipinene | 8.574 | 90.97 |
| 18 | Aromandendrene | 10.228 | 95.65 |
| 19 | 1H-Benzocycloheptene, 2,4a,5,6,7,8,9,9a-octahydro-3,5,5-trimethyl-9-methylene-, (4aS-cis)- | 10.445 | 92.52 |
| 20 | Eudesma-4(15),7-dien-1.beta. –ol | 10.766 | 98.89 |
| 21 | Diethyl chloromethanephosphonate | 10.766 | 98.41 |
| 22 | Cycloisolongifolene, 8,9-dehydro- | 10.766 | 90.88 |
| 23 | Naphthalene, 1,2,4a,5,6,8a-hexahydro-4,7-dimethyl-1-(1-methylethyl)- | 11.321 | 98.80 |
| 24 | Neoisolongifolene | 11.590 | 95.37 |
| 25 | Caryophyllene | 11.773 | 95.56 |
| 26 | .beta.-Guaiene | 11.905 | 98.65 |
| 27 | 1H-Cyclopropa[a]naphthalene, decahydro-1,1,3a-trimethyl-7-methylene-, [1aS-(1a.alpha., 3a.alpha.,7a.beta.,7b.alpha.)]- | 12.912 | 99.47 |
| 28 | Aromandendrene | 13.844 | 95.53 |
| 29 | Naphthalene, 1,2,4a,5,8,8a-hexahydro-4,7-dimethyl-1-(1-methylethyl)-, [1S-(1.alpha., 4a.beta.,8a.alpha.)]- | 14.205 | 99.37 |

**Table 2: FT-IR spectral data of responsible functional groups**

| S. No. | Frequency range ($Cm^{-1}$) | Bond type | Type of vibration | Functional group |
|---|---|---|---|---|
| 1 | 495.26 | C–Br | Stretch | alkyl halides |
| 2 | 616.51 | C–Br | Stretch | alkyl halides |
| 3 | 689.97 | –Ca” C–H: C–H | Bend | alkenes |
| 4 | 874.43 | C–H | oop | aromatics |
| 5 | 925.14 | O–H | Bend | carboxylic acids |
| 6 | 1014.44 | C–O | Stretch | alcohols, carboxylic acids, esters, ethers |
| 7 | 1062.14 | C–N | Stretch | aliphatic amines |
| 8 | 1323.74 | C–N | Stretch | aromatic amines |
| 9 | 1447.54 | C–H | Bend | alkanes |
| 10 | 2016.67 | - | - | Not known |
| 11 | 2923.79 | C–H | Stretch | alkanes |
| 12 | 3181.41 | O–H | Stretch | carboxylic acids |

**Table 3: Antibacterial assay of *I. resinosum* methanol extracts (crude)**

| Microorganisms | Zone of inhibition (mm) crude extract | | | | STD |
|---|---|---|---|---|---|
| | 25 µl | 50 µl | 75 µl | 100 µl | 25 µl |
| *Pseudomonas aeruginosa* | 08 ± 0.0 | 8.667 ± 0.577 | 10 ± 1.0 | 13 ± 1.0 | 14.667 ± 0.577 |
| *Bacillus subtilis* | 9.667 ± 1.527 | 11.667 ± 1.15 | 16 ± 1.0 | 21 ± 1.0 | 15 ± 1.0 |
| *Enterobacter* spp. | 9.667 ± 1.527 | 9.667 ± 0.577 | 13.667 ± 0.577 | 18.333 ± 0.577 | 16.333 ± 0.577 |
| *Staphylococcus aureus* | 9.667 ± 0.577 | 12.333 ± 0.57 | 15.667 ± 0.577 | 16.667 ± 0.577 | 16 ± 1.0 |
| *E. coli* | 12.667 ± 0.577 | 15.333 ± 0.57 | 16 ± 1.0 | 21 ± 1.0 | 16.333 ± 0.577 |

**Table 4: Antibacterial study of *I. resinosum* based isolated molecule**

| Microorganisms | Zone of inhibition (mm) crude extract | | | | STD |
|---|---|---|---|---|---|
| | 25 µl | 50 µl | 75 µl | 100 µl | 25 µl |
| *Pseudomonas aeruginosa* | 5.33 ± 4.618 | 8.67 ± 0.577 | 10 ± 1.0 | 12.33 ± 0.577 | 14.33 ± 0.577 |
| *Bacillus subtilis* | 9.33 ± 1.154 | 11.67 ± 0.577 | 15.67 ± 0.577 | 20.33 ± 0.577 | 15 ± 1.0 |
| *Enterobacter* spp. | 9.67 ± 1.527 | 10.33 ± 0.577 | 13.67 ± 0.577 | 18.67 ± 0.577 | 16.33 ± 0.577 |
| *Staphylococcus aureus* | 10.33 ± 0.573 | 12.67 ± 0.577 | 16.33 ± 0.577 | 17 ± 0 | 16 ± 1.0 |
| *E. coli* | 12.68 ± 0.573 | 15.33 ± 0.577 | 16 ± 1.0 | 21.33 ± 0.5773 | 15.67 ± 0.577 |

## 4. Discussion

The present study investigated the taxonomic identification, chemical profiling, and antimicrobial potential of a novel fungal specimen collected from the trunk of *Tamarindus indica* L. in the Coutrallam hills. The morphological characteristics, including the large bracket formation and distinct sulfur-yellow undersurface in young fruiting bodies, were consistent with those described for *I. resinosum*, a polypore fungus known for its ligninolytic activity and wood-decaying potential (Wang *et al.*, 2015). The specimen was successfully preserved and catalogued under the Accession Number MS-29/2019 at the SILS Herbarium. UV-Visible spectroscopy of the methanolic extract revealed multiple absorption peaks within the UV and visible spectrum (206-382 nm), indicating the presence of diverse conjugated systems and aromatic compounds. Peaks in the UV region are generally associated with $\pi \rightarrow \pi^*$ transitions in aromatic rings and $n \rightarrow \pi^*$ transitions of carbonyl groups, suggesting the presence of phenolic and other bioactive molecules (Sasidharan *et al.*, 2011). GC-MS analysis provided a comprehensive phytochemical profile of the extract, identifying 29 active compounds. These included aromatic amines, coumarins, sesquiterpenes, and other complex organic molecules with known bioactivities (Vaou *et al.*, 2021). Notably, the sesquiterpene γ-Muurolene was identified as a major constituent, previously reported for its antimicrobial and anti-inflammatory activities. The presence of these bioactive compounds suggests that *I. resinosum* may serve as a valuable source of pharmacologically relevant secondary metabolites.

Spectral characterization of γ-Muurolene was further supported by UV/Vis, FTIR, and NMR analyses. FTIR spectroscopy revealed functional groups such as alkenes, hydroxyls, and methylene stretches, which align with the molecular formula $C_2H_2$. The presence of aromatic and aliphatic protons and carbons was confirmed through $^{1}H$ and $^{13}C$ NMR, with chemical shifts consistent with previously reported data for sesquiterpenes (Silverstein and Webster, 1996). The antimicrobial assays revealed significant inhibition zones against both Gram-positive and Gram-negative bacteria. The highest activity was observed against *Bacillus subtilis* and *Escherichia coli*, suggesting broad-spectrum efficacy. The isolated compound γ-Muurolene also showed comparable antimicrobial activity, reinforcing the hypothesis that this terpenoid plays a key role in the antifungal and antibacterial defense mechanisms of the mushroom (Hossain *et al.*, 2022).

Molecular docking studies revealed strong binding affinity of γ-Muurolene to the bacterial protein EndoA (PDB ID: 6ZDF), with the top binding pose showing an affinity of -6.2 kcal/mol. This interaction was primarily driven by hydrophobic contacts with amino acid residues such as Arg143, Pro114, and Tyr120, suggesting a stable ligand-receptor complex. The favorable binding energies are indicative of potential inhibitory effects on the target protein's function, thus supporting the antimicrobial data (Morris *et al.*, 2009).While multiple docking conformations were identified, the high RMSD values of alternative poses suggest these are less stable and likely non-functional. This reinforces the specificity and strength of the top-ranked binding mode. Similar binding affinities have been observed for standard antibacterial drugs, indicating that ã-Muurolene could serve as a lead compound for the development of novel antimicrobial agents (Trott and Olson, 2010).The findings highlight *I. resinosum* as a promising source of bioactive compounds, with ã-Muurolene emerging as a key metabolite exhibiting potent antimicrobial properties. The combined morphological, chemical, and biological evidence underscores the potential of this mushroom species in natural product research and antimicrobial drug development. Further studies involving *in vivo* efficacy and molecular dynamics simulations are recommended to validate the therapeutic potential and elucidate the mechanism of action of γ-Muurolene.

## 5. Conclusion

Mushrooms are used as traditional medicine and also used as foodstuffs, cosmetics, and biocontrol agents like antibacterial, antiviral, antifungals, *etc. I resinosum* mushroom have not been well documented. The phytochemical investigation and antibacterial activity of *I. resinosum* species were studied. The methanol based extracts of *I. resinosum* had 29 phytochemical constituents were characterized by gas chromatogram and these extracts was good microbial growth inhibitor against Gram-positive and negative bacteria's like *Bacillus subtilis*, *E. coli*, *Enterobacter* spp. and *Staphylococcus aureus*. These results indicated the great antibacterial potential of the fruiting bodies of *Ischnoderma resinosum* as promising source of novel bioactive agents. The major bioactive molecule is gamma.-Muurolene have good antibacterial agent against various pathogens.

## Conflict of interest

The authors declare no conflicts of interest relevant to this article.

## References

**Abdel-Azeem, A. M.; Abdel-Azeem, M. A. and Khalil, W. F. (2019).** Endophytic fungi as a new source of antirheumatoid metabolites. In: Bioactive Food as Dietary Interventions for Arthritis and Related Inflammatory Diseases, pp:355-384. https://doi.org/10.1016/b978-0-12-813820-5.00021-0

**Basso, V.; Schiavenin, C.; Mendonça, S.; de Siqueira, F. G; Salvador, M. and Camassola, M. (2020).** Chemical features and antioxidant profile by *Schizophyllum commune* produced on different agroindustrial wastes and byproducts of biodiesel production. Food Chemistry, **329**:127089. https://doi.org/10.1016/j.foodchem.2020.127089

**Cheung, P. C. K. (1996).** The hypocholesterolemic effect of extracellular polysaccharide from the submerged fermentation of mushroom. Nutrition Research, **16** (11-12):1953-1957. https://doi.org/10.1016/S0271-5317(96)00218-7

**Ding, X. and Hou, Y. ling. (2012).** Identification of genetic characterization and volatile compounds of *Tricholoma matsutake* from different geographical origins. Biochemical Systematics and Ecology, **14**:233-239. https://doi.org/10.1016/j.bse.2012.06.003

**Ganeshpurkar, A.; Rai, G. and Jain, A. (2010).** Medicinal mushrooms: Towards a new horizon. Pharmacognosy Reviews, **4**(8):127-135. https://doi.org/10.4103/0973-7847.70904

**Gao, Z.; Kong, D.; Cai, W.; Zhang, J. and Jia, L. (2021).** Characterization and anti-diabetic nephropathic ability of mycelium polysaccharides from *Coprinus comatus*. Carbohydrate Polymers, **251**:117081. https://doi.org/10.1016/j.carbpol.2020.117081

**Gebreyohannes, G.; Nyerere, A.; Bii, C. and Berhe Sbhatu, D. (2019).** Determination of antimicrobial activity of extracts of indigenous wild mushrooms against pathogenic organisms. Evidence-Based Complementary and Alternative Medicine, **26**(1): 1-15. https://doi.org/10.1155/2019/6212673

**He, X.; Wang, X.; Fang, J.; Chang, Y.; Ning, N.; Guo, H.; Huang, L.; Huang, X. and Zhao, Z. (2017).** Structures, biological activities, and industrial applications of the polysaccharides from *Hericium erinaceus* (Lion's Mane) mushroom: A review. In International Journal of Biological Macromolecules, **97**:228-237. https://doi.org/10.1016/j.ijbiomac.2017.01.040

**Hossain, R.; Sarkar, C. and Hassan, S.M.H. (2022).** *In Silico*screening of natural products as potential inhibitors of sars-cov-2 using molecular docking simulation. Chin. J. Integr. Med., **28**:249-256. https://doi.org/10.1007/s11655-021-3504-5

**Khalilov, Q.; Li, L.; Liu, Y.; Liu, W.; Numonov, S.; Aisa, H. A. and Yuan, T. (2019).** Brassinosteroid analogues from the fruiting bodies of *Laetiporus sulphureus* and their anti-inflammatory activity. Steroids, **151**:108468. https://doi.org/10.1016/j.steroids.2019. 108468

**Kim, K.; Leem, Y.; Kim, K.; Kim, K. and Choi, H. T. (2002).** Transformation of the medicinal basidiomycete *Trametes versicolor* to hygromycin B resistance by restriction enzyme mediated integration. FEMS Microbiology Letters, **209**(2):273-276. https://doi.org/10.1016/S0378-1097(02)00555-4

**Kozarski, M.; Klaus, A.; Niksic, M.; Jakovljevic, D.; Helsper, J. P. F. G. and Van Griensven, L. J. L. D. (2011).** Antioxidative and immunomodulating activities of polysaccharide extracts of the medicinal mushrooms *Agaricus bisporus*, *Agaricus brasiliensis*, *Ganoderma lucidum* and *Phellinus linteus*. Food Chemistry, **129**(4):1667-1675. https://doi.org/10.1016/j.foodchem.2011.06.029

**Kózka, B.; Na³êcz-Jawecki, G.; Tur³o, J. and Giebu³towicz, J. (2020).** Application of *Pleurotus ostreatus* to efficient removal of selected antidepressants and immunosuppressant. Journal of Environmental Management, **273**:111131. https://doi.org/10.1016/j.jenvman.2020.111131

**Kumar, A.; Ahlawat, S.; Mohan, H. and Sharma, K. K. (2020).** Stabilization-destabilization and redox properties of laccases from medicinal mushroom *Ganoderma lucidum* and human pathogen *Yersinia enterocolitica*. International Journal of Biological Macromolecules, **167**:369-381. https://doi.org/10.1016/j.ijbiomac.2020.11.169

**Li, L. F.; Chan, B. C. L.; Yue, G. G. L.; Lau, C. B. S.; Han, Q. B.; Leung, P. C.; Liu, J. K. and Fung, K. P. (2013).** Two immunosuppressive compounds from the mushroom *Rubinoboletus ballouii* using human peripheral blood mononuclear cells by bioactivity-guided fractionation. Phytomedicine, **20**(13):1196-1202. https://doi.org/10.1016/j.phymed.2013.06.005

**Liang, C. H.; Wu, C. Y.; Lu, P. L.; Kuo, Y. C. and Liang, Z. C. (2019).** Biological efficiency and nutritional value of the culinary-medicinal mushroom *Auricularia* cultivated on a sawdust basal substrate supplement with different proportions of grass plants. Saudi Journal of Biological Sciences, **26**(2):263-269. https://doi.org/10.1016/j.sjbs.2016.10.017

**Liu, Q.; Kong, W.; Hu, S.; Kang, Y.; Zhang, Y. and Ng, T. B. (2020).** Effects of Oudemansiella radicata polysaccharide on postharvest quality of oyster mushroom (*Pleurotus ostreatus*) and its antifungal activity against *Penicillium digitatum*. Postharvest Biology and Technology, **166**:111207 https://doi.org/10.1016/j.postharvbio.2020.111207

**Marcus, J. B. (2013).** Chapter 9 - Diet and Disease: Healthy Choices for Disease Prevention and Diet Management: Practical Applications for Nutrition, Food Science and Culinary Professionals. In Culinary Nutrition.

**Mehra, A.; Narang, R.; Jain, V. K. and Nagpal, S. (2020).** Preparation and characterization of nano statins using oyster mushroom (*Pleurotus sajor-caju*): a new strategy to reduce toxicity and enhance efficacy for the treatment of cardiovascular disease. European Journal of Integrative Medicine, **33**:101014. https://doi.org/10.1016/j.eujim.2019.101014

**Morris, G.M.; Huey, R. and Lindstrom, W. (2009).** AutoDock4 and Auto Dock Tools 4: Automated docking with selective receptor flexibility. J Comput Chem., **30**:2785-2791. https://doi.org/10.1002/jcc.21256

**Nandi, A. K.; Samanta, S.; Maity, S.; Sen, I. K.; Khatua, S.; Devi, K. S. P.; Acharya, K.; Maiti, T. K. and Islam, S. S. (2014).** Antioxidant and immunostimulant â-glucan from edible mushroom *Russula albonigra* (Krombh.) Fr. Carbohydrate Polymers, **99**:774-782. https://doi.org/10.1016/j.carbpol.2013.09.016

**Reis, F. S.; Barreira, J. C. M.; Calhelha, R. C.; van Griensven, L. J. L. D.; Æiriæ, A.; Glamoèlija, J.; Sokoviæ, M. and Ferreira, I. C. F. R. (2014).** Chemical characterization of the medicinal mushroom *Phellinus linteus* (Berkeley & Curtis) Teng and contribution of different fractions to its bioactivity. LWT - Food Science and Technology, **58**(2):478-485. https://doi.org/10.1016/j.lwt.2014.04.013

**Romm, A. (2010).** Botanical Medicine for Women's Health. In: Botanical Medicine for Women's Health. https://doi.org/10.1016/B978-0-443-07277-2.X0001-3

**Sasidharan. S.; Chen, Y. and Saravanan, D. (2011).** Extraction, isolation and characterization of bioactive compounds from plants' extracts. African J. Tradit. Complement. Altern. Med. AJTCAM., **8**:1-10.

**Silverstein, R.M and Webster, F.X. (1996).** Spectrometric Identification Of Organic Compounds 6th Edition. John Wiley Sons Ltd. **6**:1-482.

**Sillapachaiyaporn, C. and Chuchawankul, S. (2020).** HIV-1 protease and reverse transcriptase inhibition by tiger milk mushroom (*Lignosus rhinocerus*) sclerotium extracts: *In vitro* and *in silico studies*. Journal of Traditional and Complementary Medicine, **10**(4):396-404. https://doi.org/10.1016/j.jtcme.2019.08.002

**Sknepnek, A.; Tomiæ, S.; Miletiæ, D.; Leviæ, S.; Èoliæ, M.; Nedoviæ, V. and Nikšiæ, M. (2020).** Fermentation characteristics of novel *Coriolus versicolor* and *Lentinus edodes* Kombucha beverages and immunomodulatory potential of their polysaccharide extracts. Food Chemistry, **342**:128344. https://doi.org/10.1016/j.foodchem.2020.128344

**Su, N. W.; Wu, S. H.; Chi, C. W.; Tsai, T. H. and Chen, Y. J. (2019).** Cordycepin, isolated from medicinal fungus *Cordyceps sinensis*, enhances radiosensitivity of oral cancer associated with modulation of DNA

damage repair. Food and Chemical Toxicology, **124**:400-410. https://doi.org/10.1016/j.fct.2018.12.025

**Szarka, C. E.; Grana, G. and Engstrom, P. F. (1994).** Chemoprevention of cancer. Current Problems in Cancer, **18**(1):6-79. https://doi.org/10.1016/0147-0272(94)90003-5

**Trott, O. and Olson, A.J. (2010).** AutoDock Vina: improving the speed and accuracy of docking with a new scoring function, efficient optimization, and multithreading. J. Comput. Chem., **31**:455-461. https://doi.org/10.1002/jcc.21334

**Vaou, N.; Stavropoulou, E. and Voidarou, C.(2021).** Towards advances in medicinal plant antimicrobial activity: A review study on challenges and future perspectives. Microorganisms, **9**:2041. https://doi.org/10.3390/microorganisms9102041

**Wang, M.; Jiang, X. and Wu, W.(2015).** Psychrophilic fungi from the world's roof. Persoonia, **34**:100-112. https://doi.org/10.3767/003158 515 X685878

**Xiao, J.; Zhang, M.; Wang, W.; Li, S.; Wang, Y.; Du, G.; Zhang, K. and Li, Y. (2020).** Using *Flammulina velutipes* derived chitin-glucan nanofibrils to stabilize palm oil emulsion: A novel food grade *Pickering emulsifier*. International Journal of Biological Macromolecules, **164**:4628-4637. https://doi.org/10.1016/j.ijbiomac.2020.09.073

**Yu, J.; Liu, C.; Ji, H.Y. and Liu, A.J. (2020).** The caspases-dependent apoptosis of hepatoma cells induced by an acid-soluble polysaccharide from *Grifola frondosa*. International Journal of Biological Macromolecules, **159**:364-372. https://doi.org/10.1016/j.ijbiomac. 2020.05.095

**Zhang, J. J.; Li, Y.; Zhou, T.; Xu, D. P.; Zhang, P.; Li, S. and Li, H. B. (2016).** Bioactivities and health benefits of mushrooms mainly from China. Molecules, **21**(7):938. https://doi.org/10.3390/molecules21070938

**Zhao, Y. and Zheng, W. (2021).** Deciphering the antitumoral potential of the bioactive metabolites from medicinal mushroom Inonotus obliquus. Journal of Ethnopharmacology, **265**:113321. https://doi.org/10.1016/j.jep.2020.113321.

**Citation** **R. Kadhar Nivas, K. Bhanumathi, C. Ramalakshmi, R. Mariselvam, S. Thanga Parameshwari and S. Ananthi (2025). Isolation and characterization of antibacterial γ-Muurolene from *Ischnoderma resinosum* (Schrad.) P. Karst.: Phytochemical analysis and efficacy against pathogenic bacteria. Ann. Phytomed., 14(1):1053-1064. http://dx.doi.org/10.54085/ap.2025.14.1.105.**